



UNIVERSITY COLLEGE LONDON

MENG MECHANICAL ENGINEERING

MECH0074 ENGINEERING IN EXTREME ENVIRONMENTS

TOPIC NOTES

Author:

HD

Module coordinator:

Prof. Ian Eames

February 8, 2023

Contents

List of Figures	3
List of Tables	4
I Extreme Pressure	5
1 Materials, Molecules and Chemistry	6
1.1 Introduction	6
1.1.1 Complexity of the problem at different length scales	6
1.1.2 Why focus on small scales?	7
1.2 Categorisation of matter	9
1.3 Atomistic view of matter	9
1.3.1 Bulk characteristic of materials	9
1.3.2 Newtonian model of matter	10
1.3.3 Vibrational modes and energy	11
1.3.4 Molecular description of material properties	11
1.3.5 Material classification	15
1.4 Kinetic theory of gases	18
1.4.1 Speed of molecules	18
1.4.2 Equations of state of real gases	18
1.5 Chemistry for engineers	20
II Extreme Temperature	21
2 How to cool very hot surfaces	22
2.1 Introduction	22
2.2 Jet engines	22
2.2.1 Brayton (or Joule) cycle	23
2.2.2 Typical values	24
2.2.3 Material selection	25
2.2.4 Manufacturing process	27
2.2.5 Thermal barrier coating	28
2.2.6 Corrosion processes	31
2.2.7 Cooling through design	32
2.3 Atmospheric re-entry objects	33
2.3.1 Idealised re-entry path	34
2.3.2 Blunt body entry vehicles	35
2.3.3 Shock layer physics	36
2.3.4 Different types of coatings	36
2.3.5 Thermal soak	37
2.3.6 Cooling methods	37

2.4 Conclusions	37
---------------------------	----

List of Figures

1.1	Pressure pulsation in a piping system	6
1.2	Graph to show complexity against scale.	7
1.3	Graph to show complexity against scale.	8
1.4	Example of plasticity from internal grain process level.	8
1.5	Hydrogen embrittlement - plastic deformation / slip	8
1.6	Rust corrosion from grain boundary level.	9
1.7	Ionic bond (electrovalence)	11
1.8	Bond stability.	11
1.9	Covalent bond (covalence). Note the overlap of electron orbit.	12
1.10	Metallic bond (electron cloud).	12
1.11	Secondary bonds. Note: long range attractive force - dipole-dipole interactions. Overlapping electron orbits - repulsive.	13
1.12	Young's modulus from atomic perspective.	14
1.13	Graph to show yield stress ratio for different materials.	15
1.14	Nucleation of crystals.	16
1.15	Stress-strain curve.	17
1.16	Toplogical changes in crystal structure.	18
1.17	Speed of molecules.	18
1.18	Van der Waals.	19
2.1	Jet engine.	22
2.2	Brayton (or Joule) cycle.	23
2.3	Typical temperature values for different stages of cycle in bypass gas-turbine engine.	24
2.4	Efficiencies of various gas-turbine engines.	25
2.5	Usage of different alloys within the engine.	26
2.6	Development of alloys.	26
2.7	Oxidation and corrosion resistance of different alloys.	27
2.8	Temperature resistance of TBCs and CMCs over the years.	28
2.9	Thermal barrier coatings (TBCs).	28
2.10	Thermal barrier coating composition.	29
2.11	Microstructure of TBC.	30
2.12	Failure of TBCs.	31
2.13	Schematic illustration of corrosive molten salts infiltration into the YSZ layer of different TBC coatings.	31
2.14	Cooling holes.	32
2.15	Blade with cooling holes.	32
2.16	Classes of cooling technologies for internal blade cooling.	33
2.17	Idealised re-entry path.	34
2.18	Re-entry path for Earth.	35
2.19	Re-entry path for Earth.	35
2.20	Shapes of entry path.	36

List of Tables

1.1	Cascade of length scales	6
1.2	Micrograph	7
1.3	Categorisation of matter	9
1.4	Key points on material properties	10
1.5	Comparison between molecular and macroscopic measurements.	14
1.6	Configurations of atoms.	16
2.1	Introduction.	22
2.2	Table to show melting points of various metals used in bypass gas-turbine engines.	24
2.3	Table to show combustion temperatures of various fuels.	24
2.4	Internal blade configurations.	33

Part I

Extreme Pressure

Chapter 1

Materials, Molecules and Chemistry

1.1 Introduction

- Macorscopic response of material depends on their microscopic structure
- We need to be able to understand physics from molecular to continuum scales

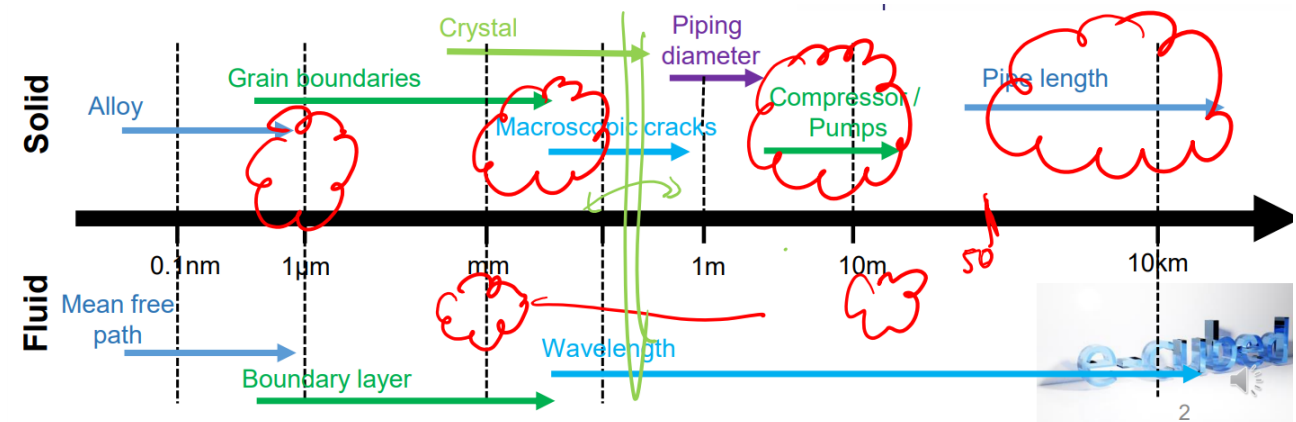


Figure 1.1: Pressure pulsation in a piping system

Cascade of length scales

1.1.1 Compelxity of the problem at different length scales

Complexity of representation changes with the scale.

Molecular	Continuum	Structural
Material is made on this level	Cracks operate on this level	Structures considered at this level
$< 10\mu\text{m}$	$10\mu\text{m} < x < 10\text{ m}$	$> 10\text{ m}$
Short range interactions	Long range interactions	Whole scale interactions
Failure / corrosion / chemistry	Tune model - variables change continuously / smoothly (can account for discontinuous behaviour, e.g. crack)	Long distance interaction - vibration (waves transporting energy)

Table 1.1: Cascade of length scales

Domain	Process
Bulk	Plasticity
Internal boundary	Hydrogen embrittlement - plastic deformation / slip
External boundary	Corrosion - chemistry

Table 1.2: Micrograph

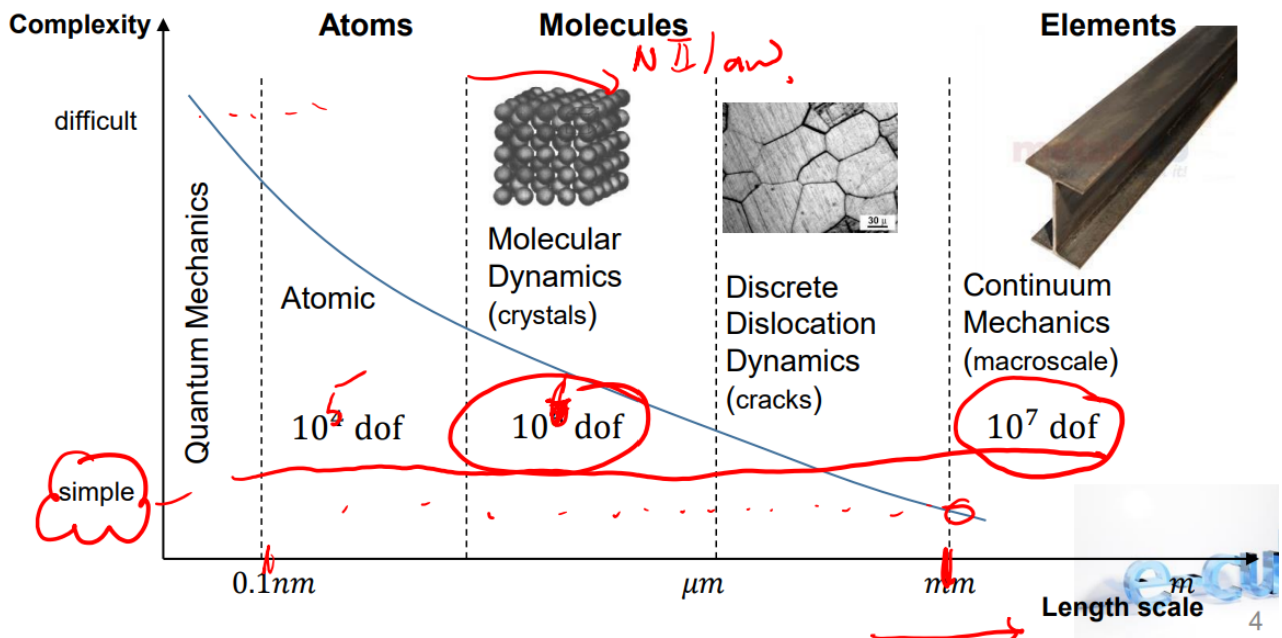


Figure 1.2: Graph to show complexity against scale.

1.1.2 Why focus on small scales?

- Small scale defects lead to crack initiation and propagation under external loading
- Failure can be corrected by changing material properties, for example, toughness
- Source of defects: complex chemical process (chemistry / corrosion) leads to corrosion at the surface
- Macroscale process is linked to microscale action
- Hypersonic flow - ionisation is non-continuum effect
- Analogy between defective liquids / solids

Note: turbulence is controlled by small vortices.

Micrograph

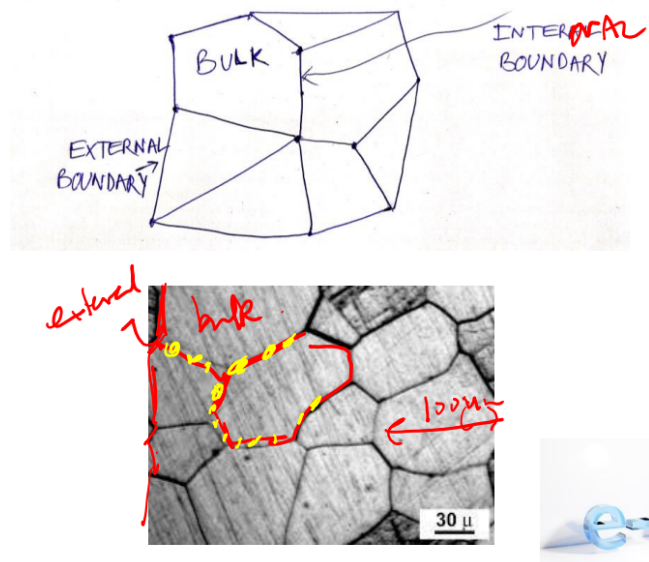


Figure 1.3: Graph to show complexity against scale.

Internal grain processes

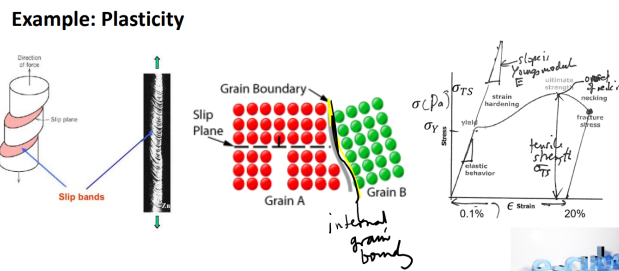


Figure 1.4: Example of plasticity from internal grain process level.

Internal boundary (hydrogen embrittlement - plastic deformation / slip)

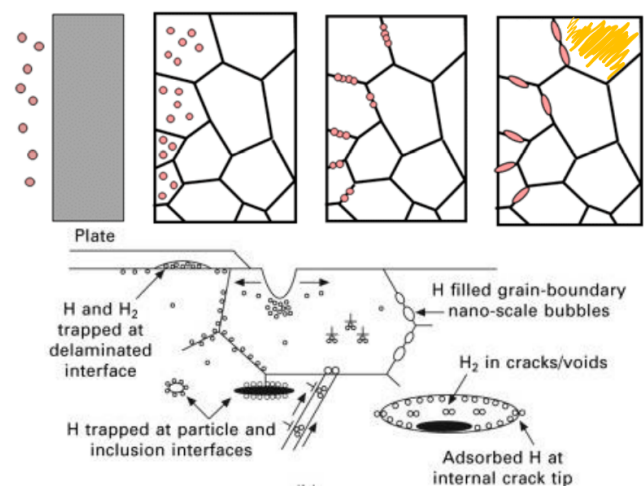


Figure 1.5: Hydrogen embrittlement - plastic deformation / slip

Matter	Modelling approach	
Solid	Atomistic	Continuum
Gas	Kinetic theory	Continuum
Liquid	Molecular	Continuum

Table 1.3: Categorisation of matter

External boundary (corrosion)

Corrosion happens over a long time and a range of scales. We need to understand how ions move around and interact with materials.

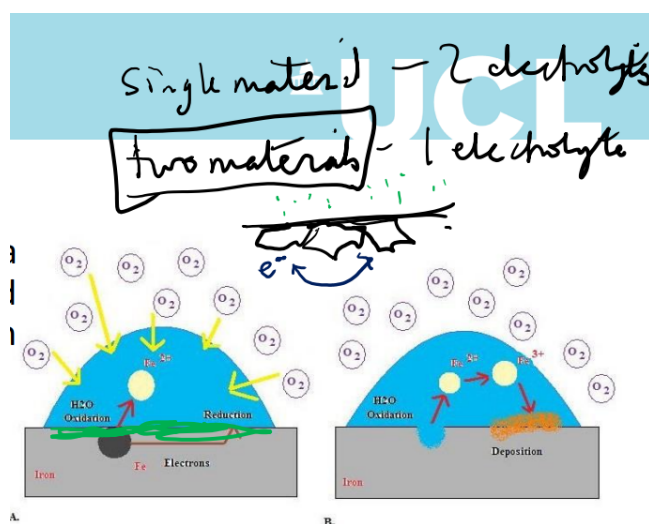
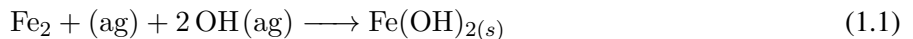


Figure 1.6: Rust corrosion from grain boundary level.

1.2 Categorisation of matter

Switch between states are due to p , V and T and is represented by phase diagram. States of matter have been part of most religious and scientific texts for the last two thousand years, with water (aqua), fire (ignis), air (aer) and earth (terra) with the fifth being the void.

1.3 Atomistic view of matter

Typical length scale:

- Diameter of atom is $0.1 \text{ nm} = 1 \times 10^{-10} \text{ m} = 1 \text{ angstrom}$
- Nucleus diameter is $1 \times 10^{-15} \text{ m}$ (hydrogen) to $15 \times 10^{-15} \text{ m}$ (uranium-238)

1.3.1 Bulk characteristic of materials

The aim is to understand the relationship between the macrostructure and the microstructure. Key measures are:

- Young's modulus $E = \frac{d\sigma}{d\varepsilon} \Big|_{\varepsilon \rightarrow 0}$

Properties		Definition
Elastic modulus	E (Pa)	Measure of material resistance to deformation.
Yield stress	σ_Y (Pa)	Measure of stress at which the elastic behaviour disappears and plastic behaviour initiates.
Hardness	HBW	Measure of material resistance to indentation
Creep		Time-dependant deformation at high temperature and constant stress.
Toughness	K (J m^{-3})	Resistance to crack propagation.
Ductility	ϵ_T	Material's ability to undergo plastic deformation.

Table 1.4: Key points on material properties

- Tensile stress: σ_{TS}
- Yields stress: σ_Y
- Ductility: ϵ_T

It is important to understand the following: How are they related to the microstrucure?

1.3.2 Newtonian model of matter

Useful for biological, physical problems, solids, liquids and gases. This is based on a description of matter as a collection of point particles, an approach that is useful for gases, liquid and solids. The dynamics of the i-th molecule is:

$$\underline{F}_i = \sum_{j,j} \neq \nabla U(x_i, x_j) \quad (1.3)$$

Located at point \underline{x}_i whose dynamics are:

$$m_i \frac{d\underline{v}_i}{dt} = \underline{F}_i \quad (1.4)$$

$$\underline{v}_i = \frac{d\underline{x}_i}{dt} \quad (1.5)$$

The formulation requires the form of the interaction stated using the Lennard-Jones 6-12 potential:

$$U = 4\epsilon \left(\left(\frac{\sigma}{r} \right)^{12} - \left(\frac{\sigma}{r} \right)^6 \right) + \dots \quad (1.6)$$

The difficultuy is that neighbourhood lists are kept and only sum over local interaction of molecules.

- Not hard collision
- Time stepping fixed
- Potentials can be empirical or chosen to now slow down calculations

$$U = U_{stretch} + U_{bend} + U_{torsion} + U_{vanderWaals} + U_{electro} + U_{cross} \quad (1.7)$$

Research gaps:

- Link between continuum and molecular
- Quantim - mechanical models

1.3.3 Vibrational modes and energy

Mechanical representation of matter. Molecules interact with their neighbours and fields. Interaction may be quite far, particularly when charges are important. We are familiar with how degrees of freedom influence properties of a gas, especially through the isentropic index. Energy is stored in various modes of vibration e.g. gas. This is called classical molecular dynamics.

1.3.4 Molecular description of material properties

Primary bonds

Ionic and covalent bonds are extremes with most (electron distribution) bonds lying between (polar covalent)

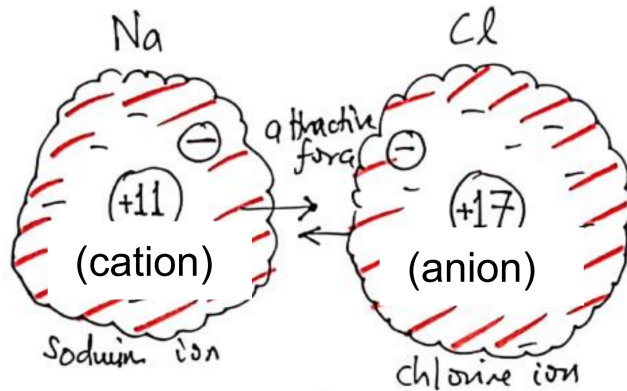


Figure 1.7: Ionic bond (electrovalence)

$$F = \frac{q_1 q_2}{4\pi\epsilon_0 r^2} \quad (1.8)$$

$$U = U_i - \frac{q^2}{4\pi\epsilon_0 r} + \frac{B}{r^n} \quad (1.9)$$

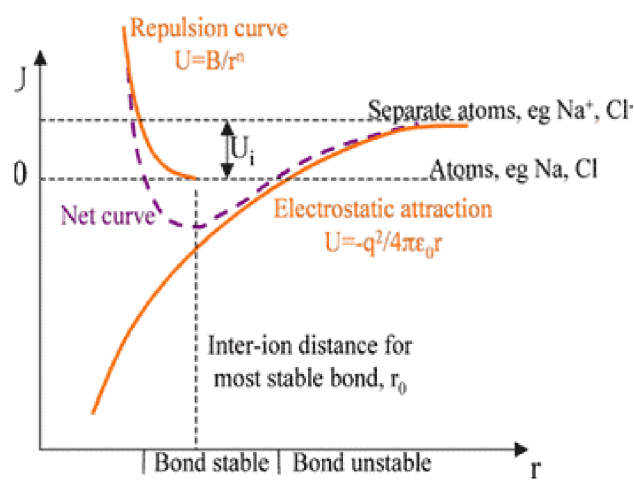


Figure 1.8: Bond stability.

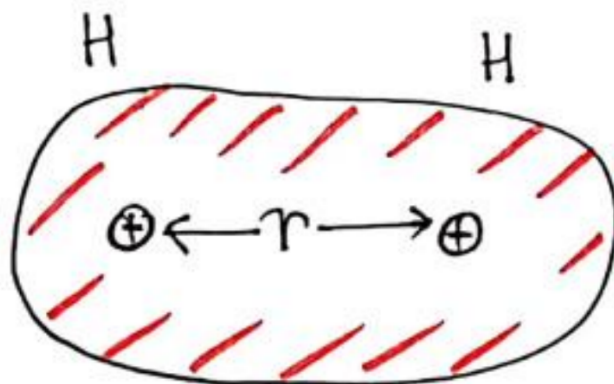


Figure 1.9: Covalent bond (covalence). Note the overlap of electron orbit.

$$U = -\frac{A}{r^m} + \frac{B}{r^n}, \quad m < n \quad (1.10)$$

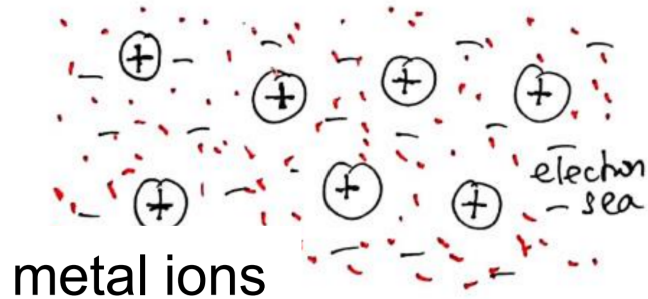


Figure 1.10: Metallic bond (electron cloud).

$$e = 1.6 \times 10^{-19} \text{ C} \quad (1.11)$$

$$\epsilon_0 = 8.8 \times 10^{-12} \text{ Nm}^2 \text{C}^{-2} \quad (1.12)$$

$$1 \text{ eV} = 1.6 \times 10^{-19} \text{ J} \quad (1.13)$$

Secondary bonds

The secondary bonds are important - without them many gases would not condense. The relative displacement of the positive and negative charge gives rise to a dipolar force. This gives rise to an attractive force. Most usual form is the Lenard Jones 6-12 potential.

$$U = -\frac{A}{r^6} + \frac{B}{r^n} \quad (1.14)$$

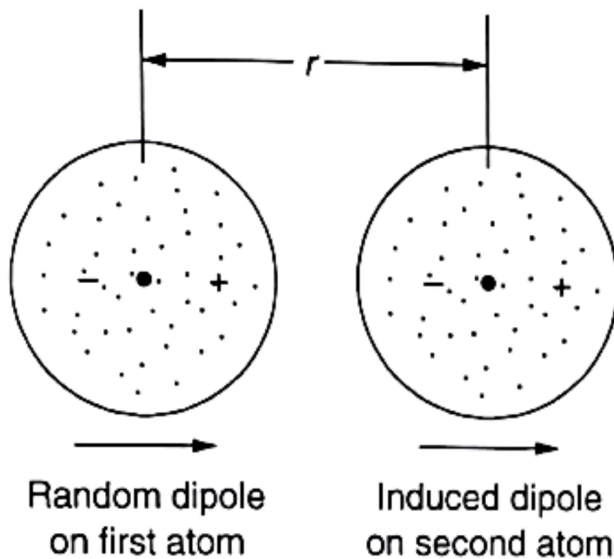


Figure 1.11: Secondary bonds. Note: long range attractive force - dipole-dipole interactions. Overlapping electron orbits - repulsive.

Physical basis of Young's Modulus

Classical mechanics:

$$m \frac{dv}{dt} = \frac{dU}{dr} \quad (1.15)$$

where U is the potential energy. At equilibrium:

$$\frac{dU}{dr} = 0 \quad (1.16)$$

so that close to this point, the energy potential can be expanded to give:

$$m \frac{d^2 r}{dt^2} = \left(\frac{d^2 U}{dr^2} \right) (r - r_0) \quad (1.17)$$

Around equilibrium point:

$$F = S_0 (r - r_0) \quad (1.18)$$

$$S_0 = - \frac{d^2 U}{dr^2} \quad (1.19)$$

The stress is:

$$\sigma = NS_0 (r - r_0) = \frac{S_0 (r - r_0)}{r_0^2} \quad (1.20)$$

The Young's modulus is:

$$E = \frac{\sigma}{\epsilon} = \frac{S_0}{r_0} \quad (1.21)$$

Estimate:

$$S_0 = \frac{\alpha q^2}{4\pi\epsilon_0 r^2} \quad (1.22)$$

$$E = \frac{\sigma}{\epsilon} = - \frac{\frac{d^2 U}{dr^2}}{r_0} = \frac{\delta e^2}{4\pi\epsilon_0 r_0^4} \quad (1.23)$$

Atom spacing:

$$\bar{r}_0 \approx 8.54$$

(1.24)

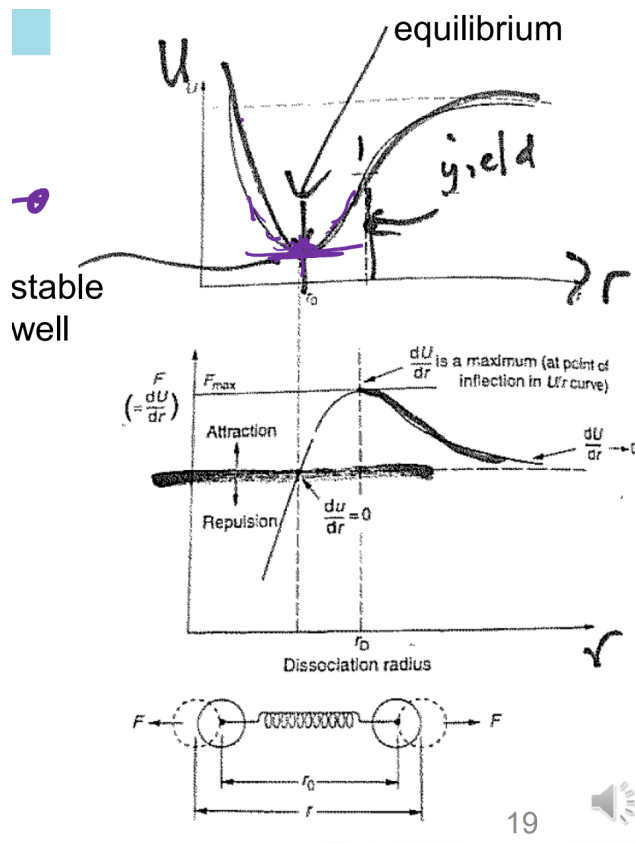


Figure 1.12: Young's modulus from atomic perspective.

Comparison between molecular and macroscopic measurements

Bond type	S_0 / Nm^{-1}	Young's modulus estimate E / GPa	Measurement
Covalent	50 - 180	200 - 1000	1000 (diamond)
Metallic	15 - 75	60 - 300	200 (nickel)
Ionic	8 - 24	32 - 96	15 - 91 (alkali halides)
H-Bond	2 - 3	8 - 12	9.1 (ice)
van der Waals	0.5 - 1	2 - 4	0.01 - 2 (rubber to nylon)

Table 1.5: Comparison between molecular and macroscopic measurements.

Estimation of yield stress

Returning to the molecular model since:

$$U = \epsilon \left(-\frac{A}{r^6} + \frac{B}{r^{12}} \right) \quad (1.25)$$

$$U'' = \epsilon \left(-\frac{6 \times 7A}{r^8} + \frac{12 \times 13B}{r^{14}} \right) \quad (1.26)$$

Then, maximum stress is:

$$\sigma_Y \approx \frac{E}{8} \quad (1.27)$$

Therefore:

$$\frac{\sigma_Y}{E} \frac{1}{8} \quad (1.28)$$

This estimated ratio is good for ceramics, but not good for metals. So what is missing from a molecular description?

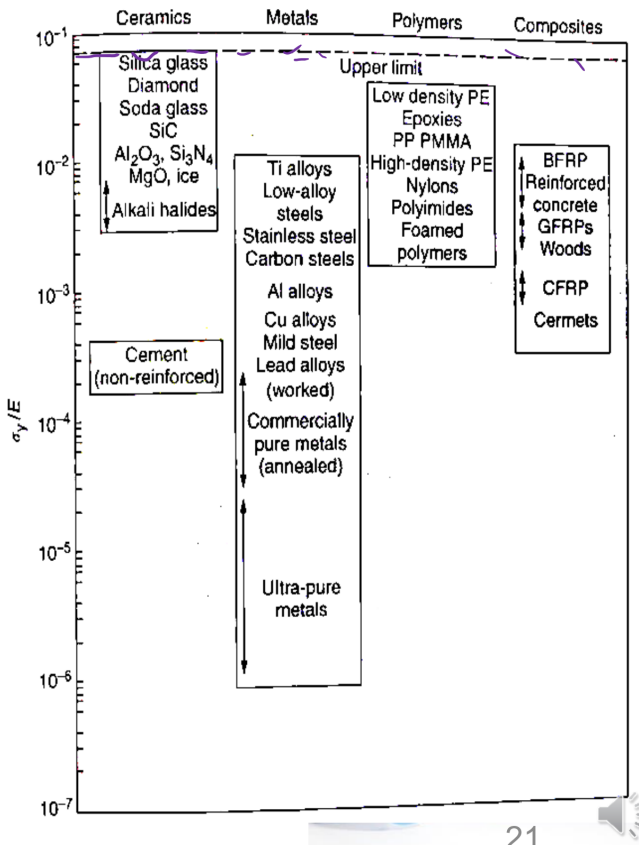


Figure 1.13: Graph to show yield stress ratio for different materials.

1.3.5 Material classification

- Metals
 - Ferrous metals and alloys
 - Non ferrous metals and alloys
 - (focus on here)
- Polymeric (non metallic, non crystalline)
 - Thermoplastic plastics
 - Thermoset plastics
 - Elastomers
- Ceramics
 - Glass
 - Diamond
 - Glass ceramics
- Composites (everything else)

- Metal-matrix composites
- Sandwich structures
- Concrete

Three common configurations

Type	Name	Description	Example
BCC	Body centred cube - 2 atoms	Harder and less malleable Packing factor 0.68	Lithium, Sodium, Potassium
FCC	Face centred cube	malleable, softer 0.74	Chromium, Barium, Alpha-iron Copper, Gold, Aluminium Iridium, Lead, Nickel, etc.
HCP	Hexagonal close packed	6 atoms Packing ratio 0.74	Cadmium, Magnesium, Titanium Zinc, Zirconium

Table 1.6: Configurations of atoms.

Solidification and crystal growth

Under normal circumstances, crystal growth starts at many nucleation points. Solidification leads to crystals growing and stop growing when they meet another crystal. A crystal is usually called a grain. The boundary between grains is the grain boundary where structure is disordered. This is controlled using nucleation points and directional solidification and liquid freezing-dendritic growth and shrinkage occurs during cooling.

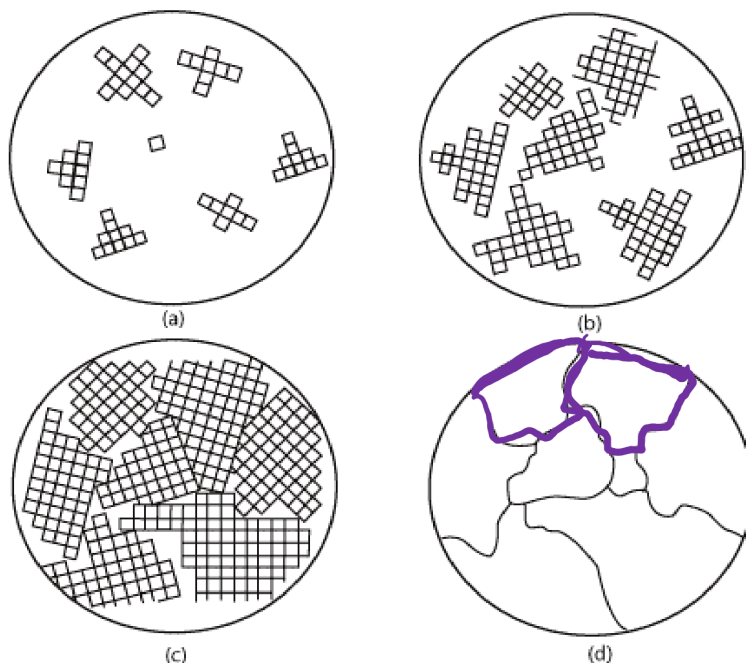


Figure 1.14: Nucleation of crystals.

Crystal defects

Three types of defects:

1. Point defects: which are places where an atom is missing or irregularly placed in the lattice structure.
Point defects include lattice vacancies, self interstitial atoms, substitution impurity atoms and interstitial impurity atoms

2. Linear defects: which are groups of atoms in irregular positions. Linear defects are commonly called dislocations
3. Planar defects: which are interfaces between homogeneous regions of the material. Planar defects include grain boundaries, stacking faults and external surfaces

Atomistic view of plastic deformation

Elastic deformation - stress is small, the metal can recover to initial state when the stress is removed. This involves stretching the bonds but atoms do not move over one another.

Plastic deformation - stress is large, plastic deformation involves the breaking of a limited number of atomic bonds by the movement of dislocations. Since the energy required to move is lowest along the densest planes of atoms, dislocations have a preferred direction of travel within a grain of the material. This results in slip that occurs along parallel planes within the grain. These parallel slip planes group together to form slip bands. A slip band appears as a single line under the microscope, but it is in fact made up of closely spaced parallel slip planes as shown in the image.

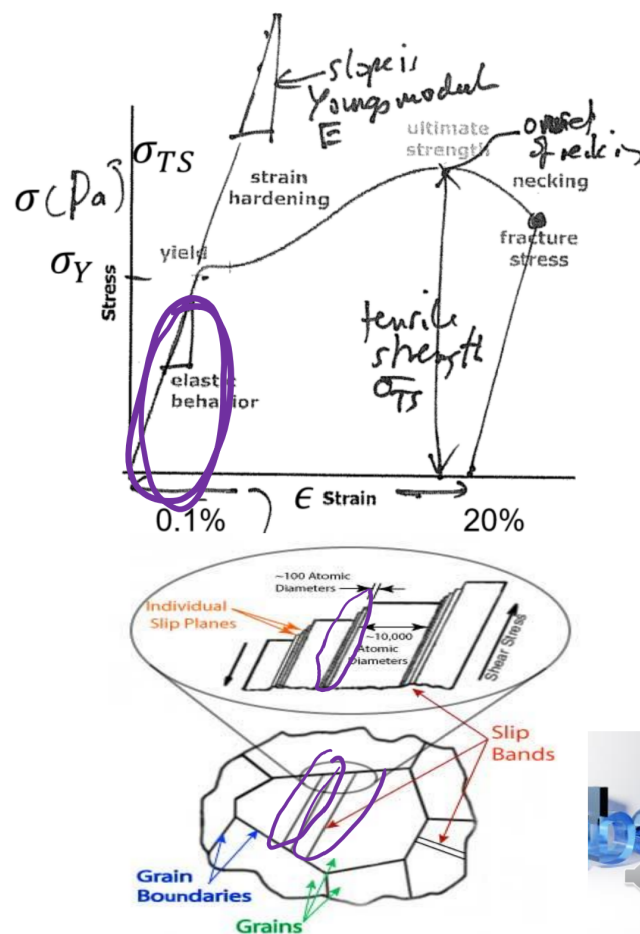


Figure 1.15: Stress-strain curve.

Fatigue crack initiation

The life of a fatigue crack has two parts, initiation and propagation. Dislocations play a major role in the fatigue crack initiation phase. It has been observed in laboratory testing that after a large number of loading cycles dislocation pile up and form structures called persistent slip bands. Initiation has a molecular origin.

Topological change in crystal structure

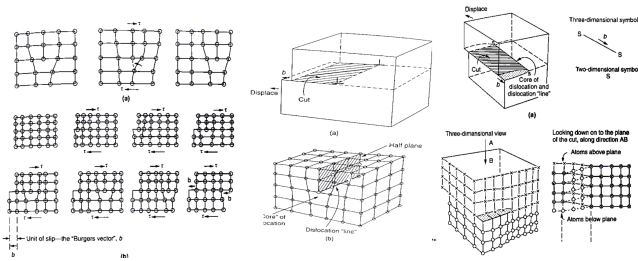


Figure 1.16: Topological changes in crystal structure.

1.4 Kinetic theory of gases

Statistical 19th century view of macroscopic properties of gas. Boltzmann and colleagues developed new techniques to describe matter. Heavily influenced the theory of turbulence ← based on kinetic theory of a gas.

$p = \rho RT$ origin with statistical theory.

This is an excellent macroscopic model of matter. The problem is that it does not work well for low pressure, high pressure or when density is low (and continuum concepts don't work).

1.4.1 Speed of molecules

Results tell us about average speed but not the distribution.

$$n_v(E) = n_0 e^{-\frac{E}{k_B T}} \quad (1.29)$$

where, $n_v(E)$ is the Boltzmann distribution which coups a lot. The speed of the molecules satisfies the Maxwell-Boltzmann distribution.

$$f(v) = 4\pi \left(\frac{m}{2\pi k_B T} \right)^{3/2} v^2 \exp \left(-\frac{mv^2}{2k_B T} \right) \quad (1.30)$$

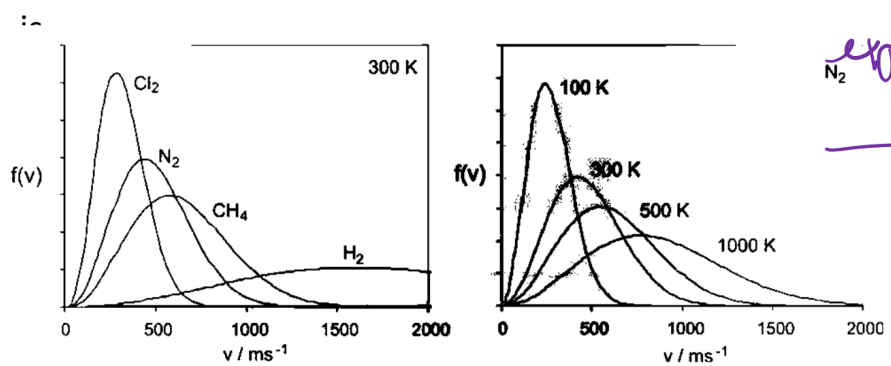


Figure 1.17: Speed of molecules.

1.4.2 Equations of state of real gases

The molecular continuum view of matter are linked. Virial equation:

$$pV = nRT \left(1 + \frac{B}{V_m} + \frac{C}{V_m^2} + \dots \right) \quad (1.31)$$

where B, C are the second and third virial coefficients. Van der Waals equation:

$$\left(p + a \frac{n^2}{V^2} \right) (V - nb) = nRT \text{ or} \quad (1.32)$$

$$P = \frac{nRT}{V - nb} - a \frac{n^2}{V^2} \quad (1.33)$$

n is the number of moles. nb is the volume excluded since molecules cannot overlap. $\frac{an^2}{V^2}$ pressure reduced due to attractions between pairs of molecules.

Critical constants for van der Waals equation

Solving these two equations in two unknowns (temperature and molar volume) gives the critical temperature and critical molar volume:

$$T_c = \frac{8a}{27Rb} \quad (1.34)$$

$$V_c = 3b \quad (1.35)$$

Van der Waals

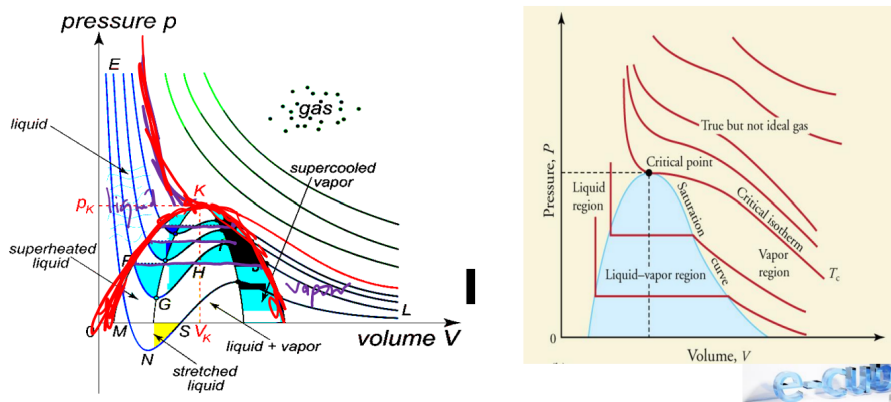


Figure 1.18: Van der Waals.

Link between molecular and microscopic

Most of the important 19th century breakthroughs were determining link between macroscopic (could be seen) and microscopic (could not be seen). For example, Brownian motion:

$$\frac{RT}{5\pi\mu dN_A} = D = \lim_{t \rightarrow \infty} \frac{(x^2)}{2t} \approx 10 \times 10^{-10} \text{ m}^2 \text{ s}^{-1} \quad (1.36)$$

This represented a link between Avogadro's constant and macroscopic movement of particles. Here $N_A = 6 \times 10^{23} \text{ mol}^{-1}$. Theory by Einstein (1905) and Sutherland (1905). Millikan's experiments: determination of the charge on an electron. The link between molecular and microscopic last areas of modern science to be worked out.

Einstein theory and Millikan's experiment

Based around kinetic theory of gases and momentum change due to collision. Pressure is a manifestation of a:

$$P = \frac{2}{3} \frac{N}{V} \frac{1}{2} m_0 \bar{v}^2 \quad (1.37)$$

$$\therefore PV = nRT = \frac{N}{N_a} RT = Nk_B T \quad (1.38)$$

$$\therefore KE = \frac{3}{2} N k_B T = \frac{3}{2} nRT = \frac{NDF}{2} nRT \quad (1.39)$$

where NDF is number of degrees of freedom.

Model assumptions

- No intermolecular forces between the gas particles
- The volume occupied by the particles is negligible compared to the volume of the container they occupy
- The only interactions between the particles and with the container walls are perfectly elastic collisions.
- Real gas, the atoms or molecules have a finite size, and at close range they interact with each other through a variety of intermolecular forces, including dipole-dipole interactions, dipole induced dipole interactions and van der Waal's (induced dipole - induced dipole) interactions
- When applied to real gases, the ideal gas model breaks down when molecular size effects or intermolecular forces become important. This occurs under conditions of high pressure , where the molecules are forced close together and therefore interact strongly, and at low temperatures, when the molecules are moving slowly and intermolecular forces have a long time to act during a collision

The pressure at which the ideal gas model starts to break down will depend on the nature and strength of the intermolecular forces between the gas particles, and therefore on their identity. The ideal gas model becomes more and more exact as the pressure is lowered, since at very low pressures the gas particles are widely spaced apart and interact very little with each other.

$$\text{number density} = \frac{N}{V} = \frac{nN_A}{V} \quad (1.40)$$

$$\Delta p_x = (2mv_x) \left(\frac{1}{2} \frac{nN_A}{V} Av_x \Delta t \right) = \frac{nMAv_x^2 \Delta t}{V} \quad (1.41)$$

$$p = \frac{F_x}{A} = \frac{nMv_x^2}{V} \quad (1.42)$$

1.5 Chemistry for engineers

Chemistry has a molecular origin. The engineering challenge is how to include chemistry into multiphysics problems. Chemistry might be simple:



Part II

Extreme Temperature

Chapter 2

How to cool very hot surfaces

2.1 Introduction

Context	Material development	Design
Gas turbine engines	Material development manufacturing techniques	TBC air cooling
Re-entry spacecraft	Surface properties ablation	Angle of attack changing geometry
Silicon processors	None really - still with silicon with an adhesive metal plate	Clamp on cooling system

Table 2.1: Introduction.

2.2 Jet engines

Purpose is to convert chemical energy into linear momentum (IC engine - chemical energy into pressure).

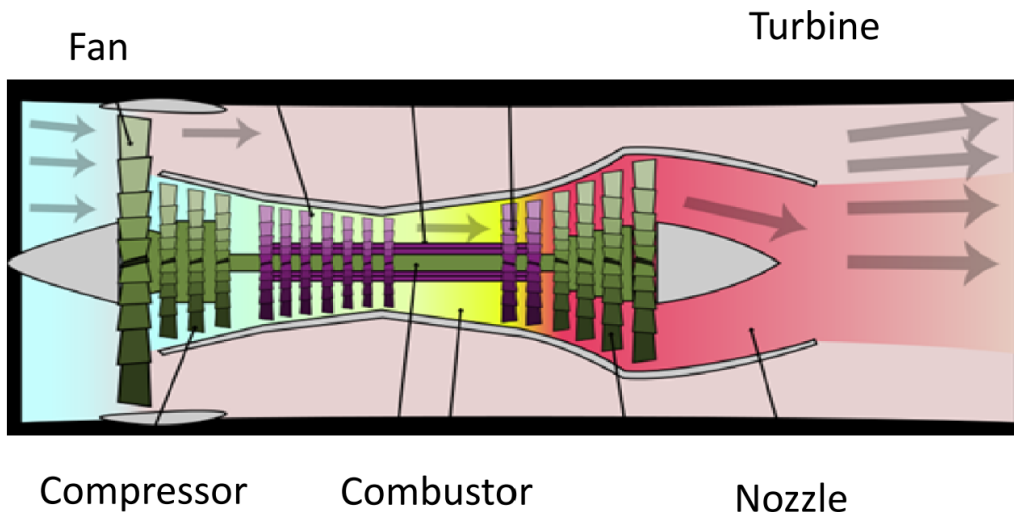


Figure 2.1: Jet engine.

2.2.1 Brayton (or Joule) cycle

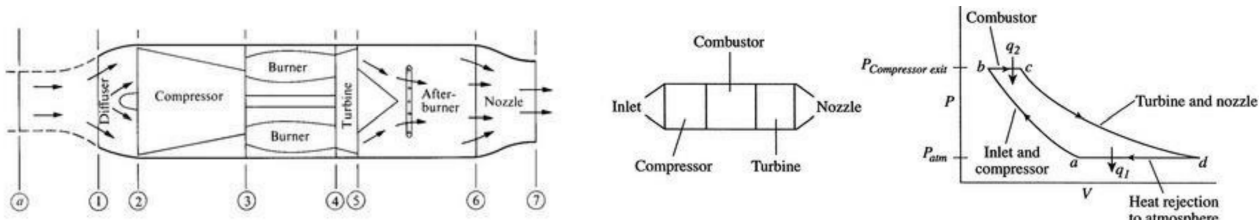


Figure 2.2: Brayton (or Joule) cycle.

- a-b: adiabatic, quasi-static (or reversible) compression in the inlet and compressor
- b-c: constant pressure fuel combustion (idealised as constant pressure heat addition)
- c-d: adiabatic, quasi-static (or reversible) expansion in the turbine and exhaust nozzle, with which we take some work out of the air and use it to drive the compressor and take the remaining work out and use it to accelerate fluid for jet propulsion, or to turn a generator for electrical power generation
- d-a: cool the air at constant pressure back to its initial condition
- **Fan** - the large spinning fan sucks in large quantities of air. It then speeds this air up and splits it into two parts. One part continues through the “core” or centre of the engine, where it is acted upon by the other engine components. The second part “bypasses” the core of the engine. It goes through a duct that surrounds the core to the back of the engine where it produces much of the force that propels the airplane forward. The cooler air helps to quiet the engine as well as adding thrust to the engine.
- **Compressor** - the compressor is the first component in the engine core. The compressor squeezes the air that enters it into progressively smaller areas, resulting in an increase in the air pressure. This results in an increase in the energy potential of the air. The squashed air is forced into the combustion chamber.
- **Combustor** - in the combustor the air is mixed with fuel and then ignited. This provides a high temperature, high-energy airflow. The fuel burns with the oxygen in the compressed air, producing hot expanding gases. The inside of the combustor is often made of ceramic materials to provide a heat-resistant chamber. The temperature can reach 2700 °C
- **Turbine** - the high-energy airflow coming out of the combustor goes into the turbine, causing the turbine blades to rotate. The turbines are linked by a shaft to turn the blades in the compressor and spin the intake fan at the front. This rotation takes some energy from the high-energy flow that is used to drive the fan and the compressor. The gases produced in the combustion chamber move through the turbine and spin its blades. The turbines of the jet spin around thousands of times. They are on fixed shafts which have several sets of ball-bearings in between them.
- **Nozzle** - the nozzle produces the thrust for the plane. The energy depleted airflow that passed the turbine in addition to the colder air that bypassed the engine core, produces a force when exiting the nozzle that acts to propel the engine, and therefore the airplane, forward. The combination of the hot air and cold air are expelled and produce an exhaust, which causes a forward thrust. The nozzle may be preceded by a mixer, which combine the high temperature air coming from the engine core with the lower temperature air that was bypassed in the fan. The mixer helps to make the engine quieter.

2.2.2 Typical values

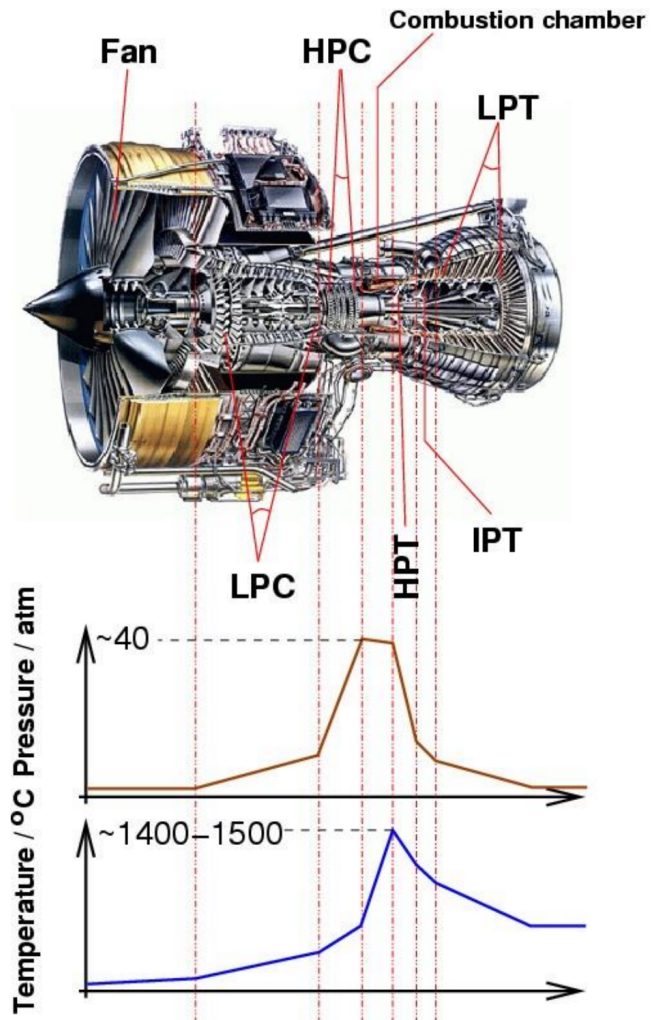


Figure 2.3: Typical temperature values for different stages of cycle in bypass gas-turbine engine.

Metal	Melting point
Titanium	1668 °C
Nickel	1455 °C
Steel	1370 °C

Table 2.2: Table to show melting points of various metals used in bypass gas-turbine engines.

Combustion at about 1800-1900 °C. Large centrifugal acceleration 25 000 rpm for large engines 500 000 rpm for micro gas turbine. Higher temperature makes the thermodynamic efficiency greater (about 60%). Combustion temperature is above melting point of metals.

Fuel	Combustion temperature
Methane (in air)	1950 °C
Hydrogen (in air)	2110 °C
Propane (in oxygen)	2880 °C

Table 2.3: Table to show combustion temperatures of various fuels.

Meeting the needs

1. Choice of material
2. Manufacturing technique
3. Design

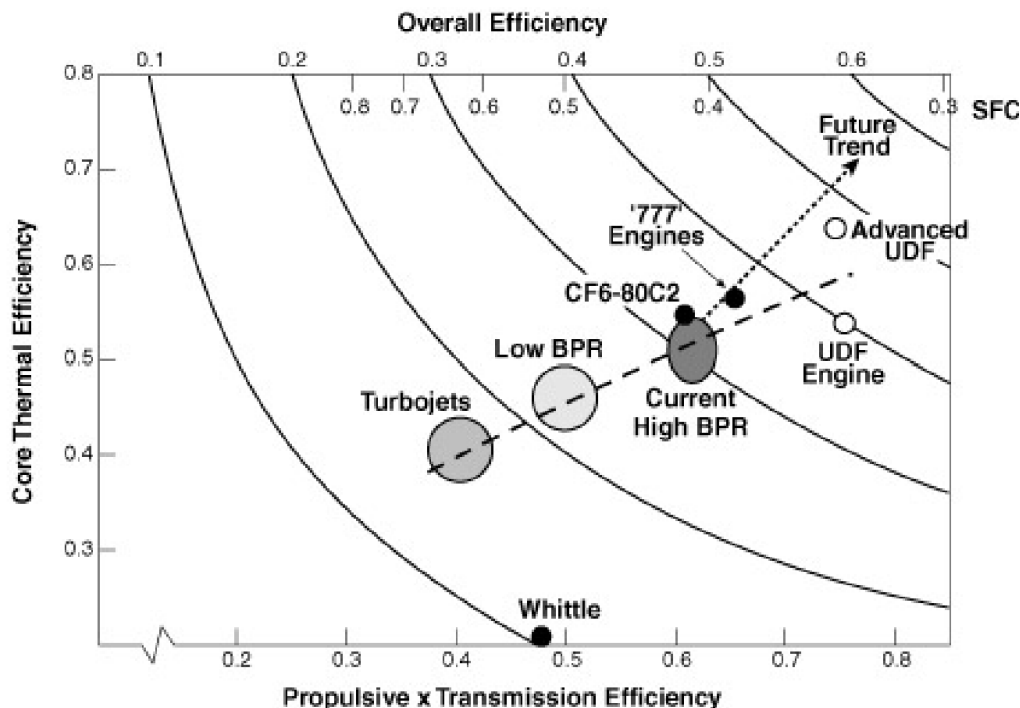


Figure 2.4: Efficiencies of various gas-turbine engines.

2.2.3 Material selection

Considerations:

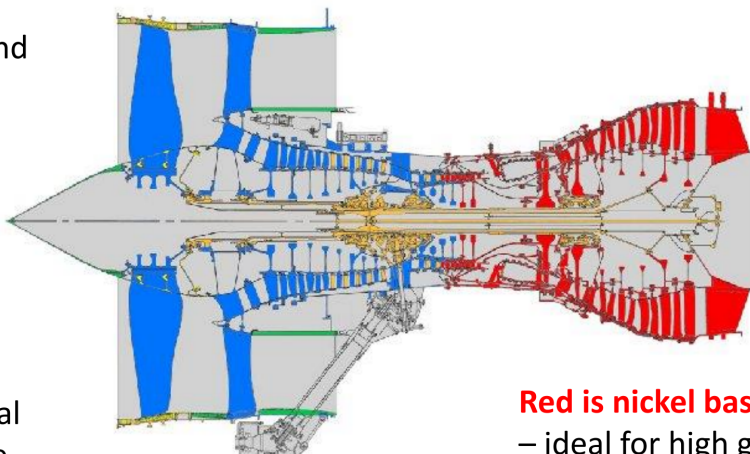
1. Strength and weight: titanium
2. Temperature: major constraint is the material selection for the hot section (combustor and turbine) of the engine

The need for better materials spurred much research in the field of alloys and manufacturing techniques, and that research resulting in a long list of new materials and methods that make modern gas turbines possible. One of the earliest of these was Nimonic 90 (nickel-based, high-temperature, low-creep superalloys Ni 54%, Cr 18-21%, Co 15-21%, Ti 2-3%, Al 1-2%).

The development of superalloys in the 1940s and new processing methods such as vacuum induction melting in the 1950s greatly increased the temperature capability of turbine blades. Further processing methods like hot isostatic pressing improved the alloys used for turbine blades and increased turbine blade performance. Modern turbine blades often use nickel-based superalloys that incorporate chromium, cobalt and rhenium.

Blue is titanium –

ideal for strength and density and low temperatures



Orange – steel – ideal for static parts of the compressor high temperature.

Red is nickel based superalloys

- ideal for high gas temperature
- entrance temperature is 1400°C , cooling system (surface temp 1100°C) with coating is 930°C

Figure 2.5: Usage of different alloys within the engine.

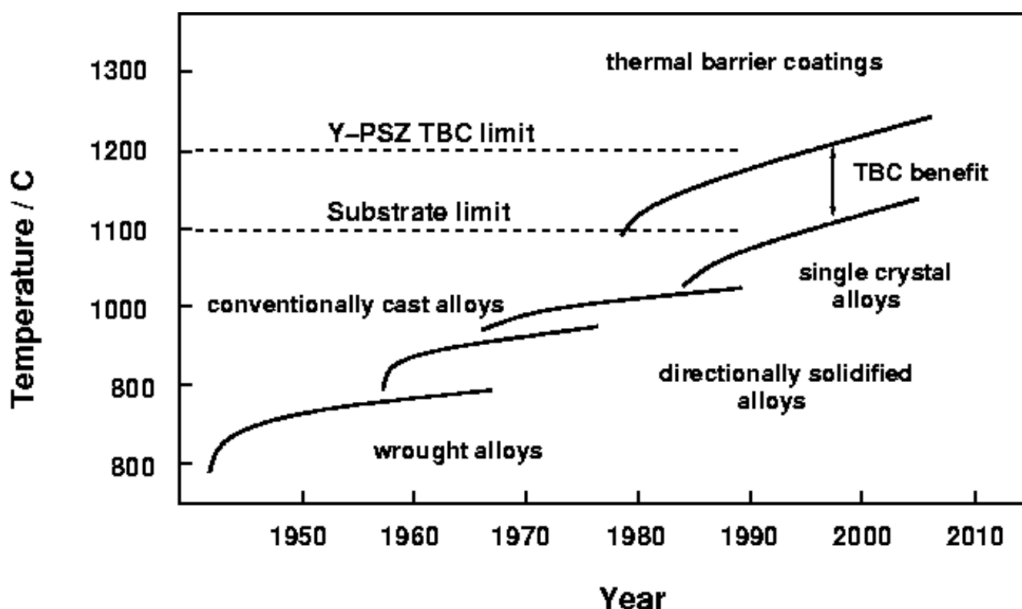


Figure 2.6: Development of alloys.

Titanium - good for weight and strength (poor with heat).

Alloy improvement, directional and single-crystal solidification have contributed significantly, but arguably, the emphasis has been shifted to coating systems which have allowed an increase of gas temperatures up to 1100°C . Coatings in gas turbines serve a variety of purposes. A first requirement to operate turbines at higher temperatures was, of course, improved strength. Unfortunately, these conditions also mean severe oxidation / corrosion problems, and to make things worse, the improvement in mechanical properties of the base alloys was made at the expense of environmental resistance.

The first purpose of coatings was to improve poor oxidation resistance of the base alloy (aluminide, Pt-aluminide, MCrAlY). A second type of coatings applied to high-temperature parts are known as thermal barrier coatings (TBC). These are ceramic coatings with very low thermal conductivity and thin ($200\ \mu\text{m}$). Drop of $100\text{--}300^{\circ}\text{C}$ between the gas and metal surface temperatures but are ‘oxygen transparent’ and do not prevent

oxidation of the underlying substrate.

2.2.4 Manufacturing process

Aside from the alloy improvements, a major breakthrough was the development of directional solidification (DS) and single crystal (SC) production methods. These methods help greatly increase strength against fatigue and creep by aligning grain boundaries in one direction (DS) or by eliminating grain boundaries altogether (SC).

Recent generations of superalloys for single crystal turbine blades contain relatively high percentages of refractory elements such as Ta, W or Re which enhance the high-temperature mechanical properties.

This is done at the expense of Cr and Al. Given the severe environmental conditions in which the blades operate, the removal of the elements (beneficial for oxidation resistance) implies even greater degradation problems.

To reduce the oxidation corrosion resistance, an external coating is applied to the blades. Its purpose is to allow for the growth of a resistant oxide layer. Of all possible oxides $\alpha\text{-Al}_2\text{O}_3$ offers excellent protection and very low growth rates (in a minority of cases, Cr oxides are preferred). The composition of the coating must therefore be chosen carefully so as to ensure growth of $\alpha\text{-Al}_2\text{O}_3$.

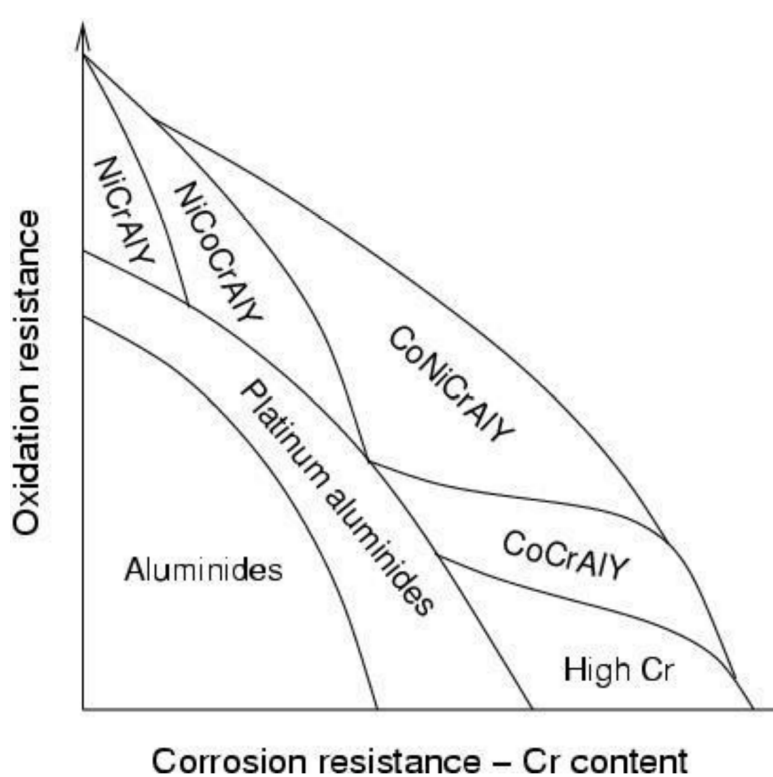


Figure 2.7: Oxidation and corrosion resistance of different alloys.

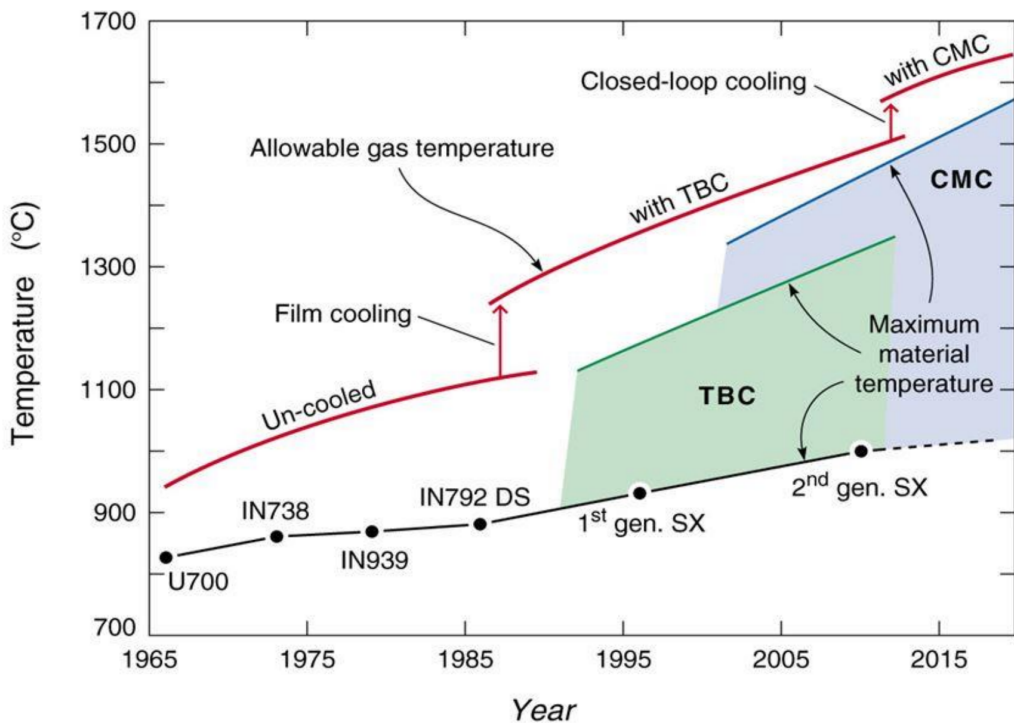


Figure 2.8: Temperature resistance of TBCs and CMCs over the years.

TBC - thermal barrier coating. CMC - ceramic matrix composite.

2.2.5 Thermal barrier coating

Thermal barrier coatings (TBC) are advanced materials systems usually applied to metallic surfaces, such as on gas turbine or aero-engine parts, operating at elevated temperatures, as a form of exhaust heat management. These 100 µm to 2 mm coatings serve to insulate components from large and prolonged heat loads by utilising thermally insulating materials which can sustain an appreciable temperature difference between the load-bearing alloys and the coating surface.

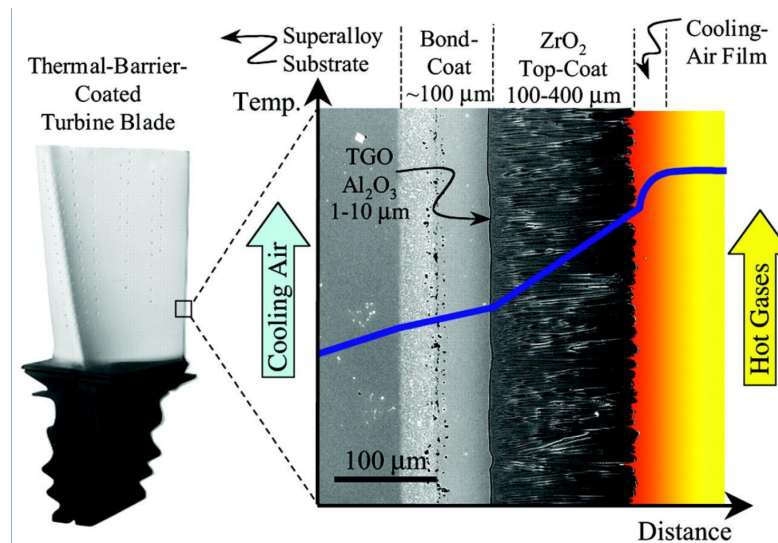


Figure 2.9: Thermal barrier coatings (TBCs).

Four layers:

1. The metal substrate

2. Metallic bond coat
3. Thermally-grown oxide (TGO)
4. Ceramic topcoat. The ceramic topcoat is typically composed of yttria-stabilised zirconia (YSZ) which is desirable for having very low of conductivity while remaining stable at nominal operating temperatures typically seen in applications. This ceramic layer creates the largest thermal gradient of the TBC and keeps the lower layers at a lower temperature than the surface.

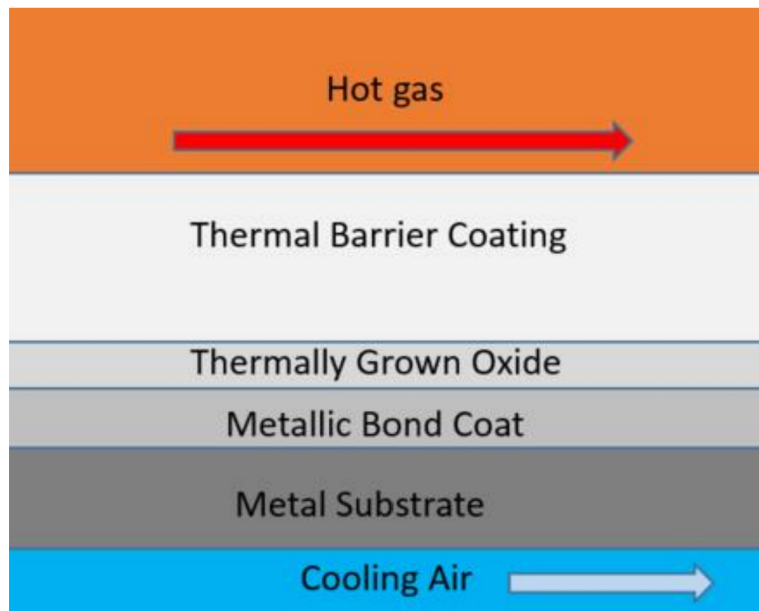


Figure 2.10: Thermal barrier coating composition.

TBCs improved corrosion and oxidation resistance, both of which became greater concerns as temperatures increased. First TBCs (1970s) were aluminide coatings. Ceramic coatings in 1980s which decreased turbine blade temperature by about 90 °C, improve blade life, almost doubling the life of turbine blades in some cases.

An effective TBC needs to meet certain requirements to perform well in aggressive thermo-mechanical environments. To deal with thermal expansion stresses during heating and cooling, adequate porosity is needed, as well as appropriate matching of thermal expansion coefficients with the metal surface that the TBC is coating.

1. A high melting point
2. No phase transformation between room temperature and operating temperature
3. Low thermal conductivity
4. Chemical inertness
5. Similar thermal expansion match with the metallic substrate
6. Good adherence to the substrate
7. Low sintering rate for a porous microstructure

These requirements severely limit the number of materials that can be used, with ceramic materials usually being able to satisfy the required properties.

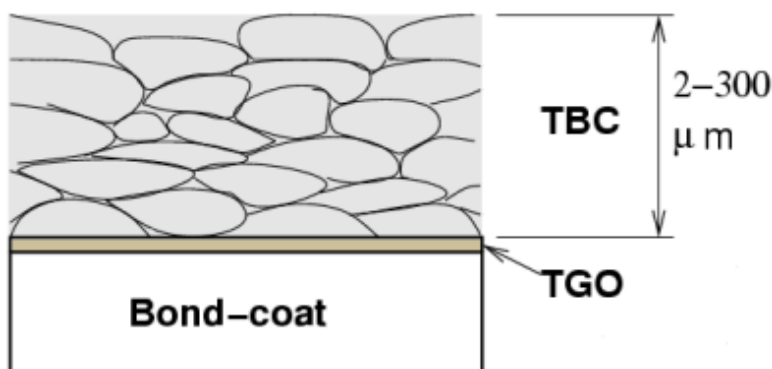


Figure 2.11: Microstructure of TBC.

For a ceramic coating to have any chance not to spall at the first thermal cycle, it is critical that its thermal expansion be close to that of the substrate. For the coating to be of use, it must also exhibit a very low thermal conductivity.

Thermal barrier coatings typically consist of four layers: the metal substrate, metallic bond coat, thermally-grown oxide (TGO), and ceramic topcoat. The ceramic topcoat is typically composed of yttria-stabilised zirconia (YSZ) which is desirable for having very low thermal conductivity while remaining stable at nominal operating temperatures typically seen in applications. This ceramic layer creates the largest thermal gradient of the TBC and keeps the lower layers at a lower temperature than the surface.

Most turbine blades are manufactured by investment casting (or lost-wax processing). This process involves making a precise negative die of the blade shape that is filled with wax to form the blade shape. If the blade is hollow (i.e. it has internal cooling passages), a ceramic core in the shape of the passage is inserted into the middle. The wax blade is coated with a heat-resistant material to make it a shell, and then that shell is filled with the blade alloy. This step can be more complicated for DS or SC materials, but the process is similar. If there is a ceramic core in the middle of the blade, it is dissolved in a solution that leaves the blade hollow. The blades are coated with a TBC, and then any cooling holes are machined. Ceramic matrix composites (CMC), where fibres are embedded in a ceramic matrix, are being developed for use in turbine blades. Main advantage of CMCs over conventional superalloys is their light weight and high temperature capability. SiC/SiC composites consisting of silicon matrix reinforced by silicon carbide fibres have been shown to withstand operating temperatures 100-200 °C higher than nickel superalloys.

Coating failure

TBCs fail through various degradation modes that include mechanical rumpling of bond coat during thermal cyclic exposure, especially coatings in aircraft engines; accelerated oxidation, hot corrosion, molten deposit degradation. There are also issues with oxidation (areas of the TBC getting stripped off) of the TBC, which reduces the life of the metal drastically, which leads to thermal fatigue.

A key feature of all TBC components is well matched thermal expansion coefficients between all layers. TBCs expand and contract at different rates upon heating and cooling of the environment, so when the different layers have poorly thermal expansion coefficients, a strain is introduced in the material which can lead to cracking and ultimately failure of the coating.

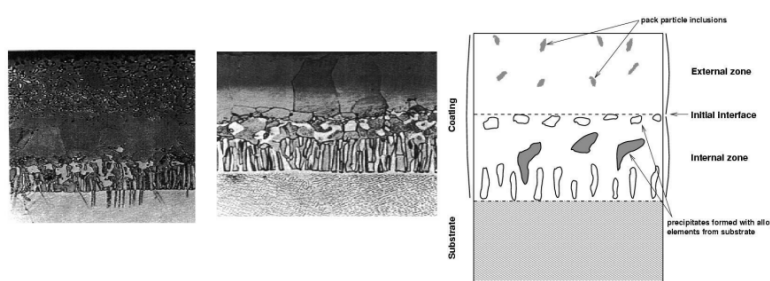


Figure 2.12: Failure of TBCs.

2.2.6 Corrosion processes

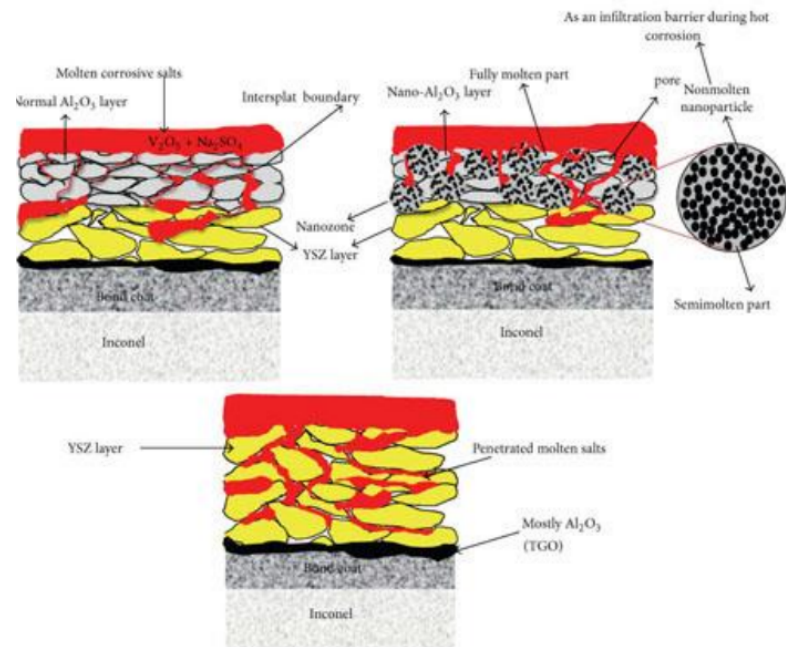


Figure 2.13: Schematic illustration of corrosive molten salts infiltration into the YSZ layer of different TBC coatings.

The high-pressure turbine of a jet turbine provides one of the most severe environments faced by man-made materials. To temperatures approaching the substrate melting point, one must add the considerable stresses caused by rotation at more than 10 000 rpm. Thermal barrier coating failure results in melting of the blade. Without reaching such catastrophic failure, blades suffer from accelerated oxidation or hot corrosion. Coatings can considerably enhance the oxidation/hot corrosion resistance of these components. Oxidation is the reaction between the coating (or in its absence, base alloy) with the oxidants present in the hot gases. Hot corrosion occurs from surface reactions with salts deposited from the vapour phase. This is caused by diffusion through the substrate alloy, as they are not in thermodynamic equilibrium with the latter.

2.2.7 Cooling through design

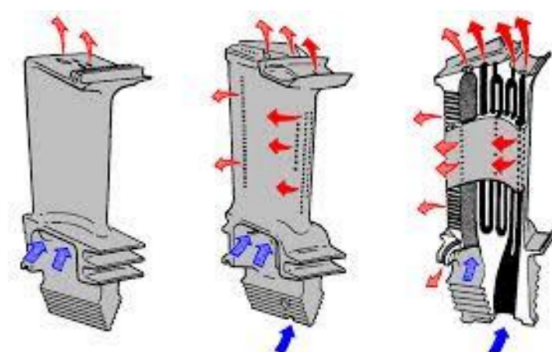
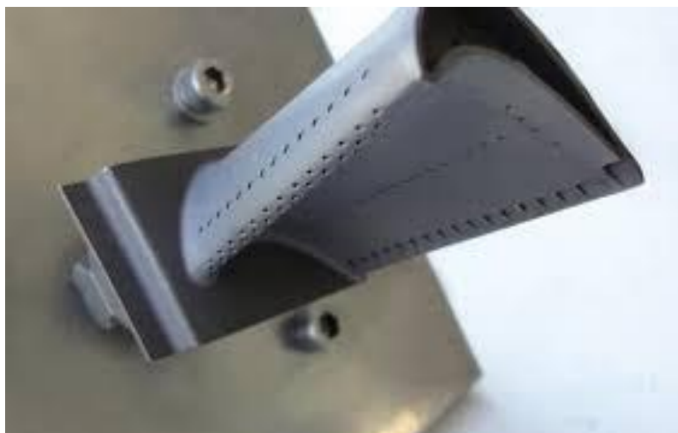


Figure 2.14: Cooling holes.



Figure 2.15: Blade with cooling holes.

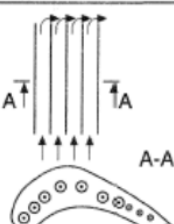
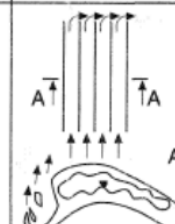
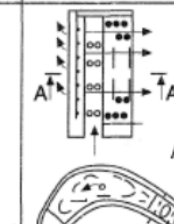
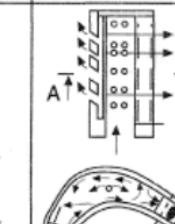
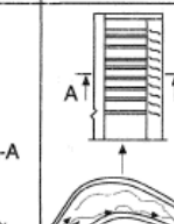
Main Data	Engine Type				
	JT8D-11(15)	JT9D-3A	JT9D-7	JT9D-59/70D	F-100
Tg, K	1294~1340	1420	1500	1598...1643	1590...1672
δ, %	~1,0	1,96	2.1	3.4	-3.0
θ	-0.2	-0.3	-0.45	-0.5	-0.55
Cooling system development	 Radial air flow ducts Multiflow - line schematic diagram of air flow	 Radial air flow ducts	 Deflector blade with air jet stream	 Film cooling and cooling air twisting 1.3% 1 + 2	 1. Deflector blade welded from two parts 2. Cooling air twisting 3. Development surface of inner finning

Table 2.4: Internal blade configurations.

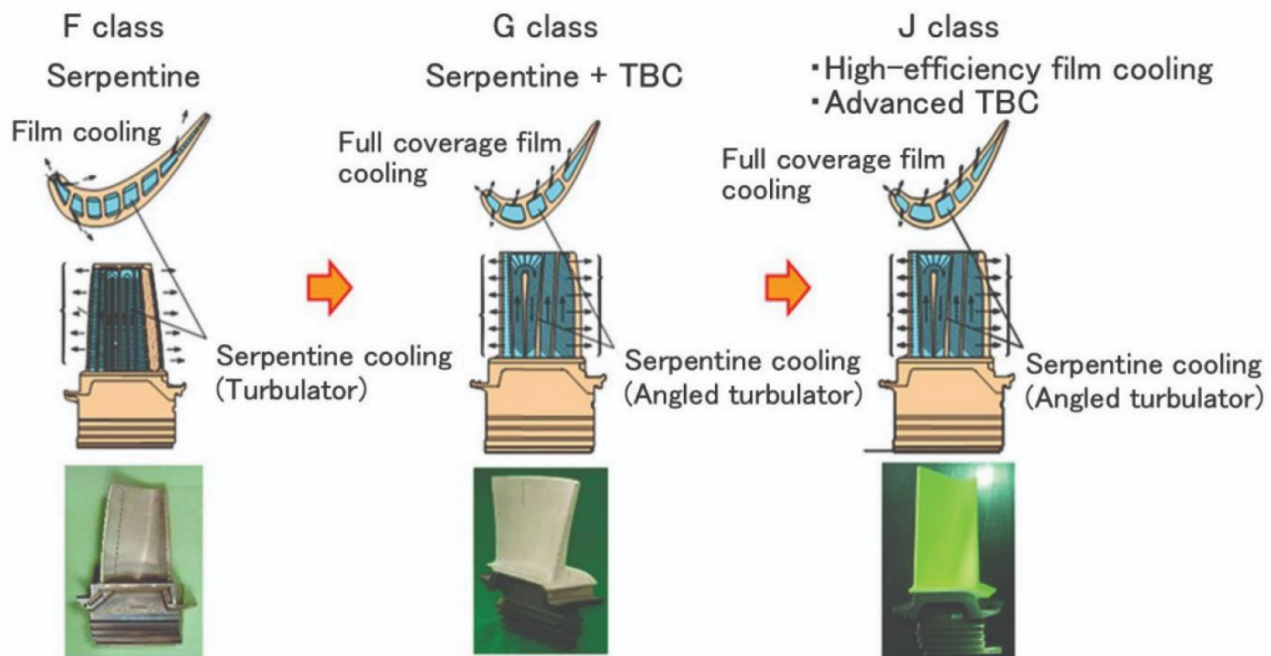


Figure 2.16: Classes of cooling technologies for internal blade cooling.

2.3 Atmospheric re-entry objects

Two types of entry:

1. Uncontrolled
2. Controlled (or EDL entry, descent and landing)

The kinetic energy of re-entry vehicles is enormous (50-1800 GJ) and thus must be expended. This is because this is the potential energy that must be lost. It is not possible to use retro rockets over whole descent as this uses too much fuel. Most objects require slowing down (except for ballistic warheads).

2.3.1 Idealised re-entry path

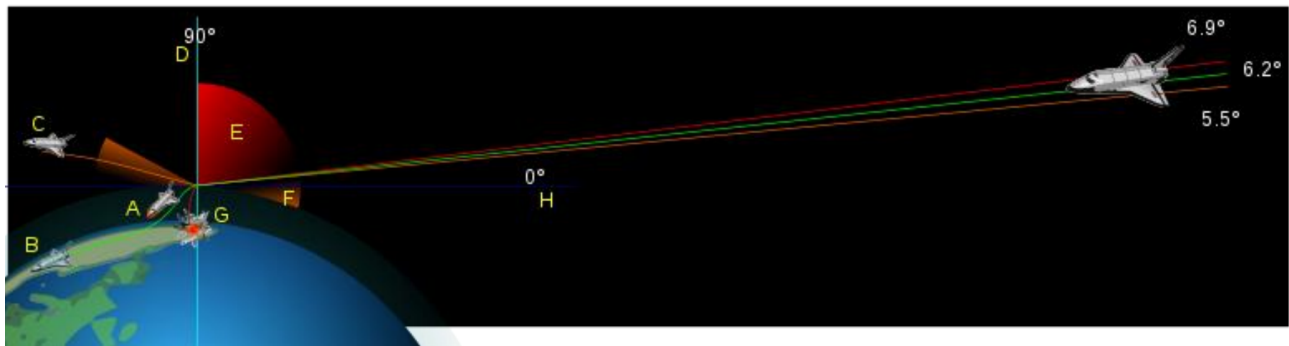


Figure 2.17: Idealised re-entry path.

Re-entry window:

- A - friction with air
- B - in air flight
- C - expulsion lower angle
- D - perpendicular to the entry point
- E - excess friction 6.9° to 90°
- F - repulsion of 5.5° or less
- G - explosion friction
- H - plane tangential to the entry point

Karman line

- Earth - 100 km
- Venus - 250 km
- Mars - 80 km

Most objects enter at hypersonic speeds. Alternative on planets with thick atmospheres or strong gravity - Venus, Titan and the gas giants.

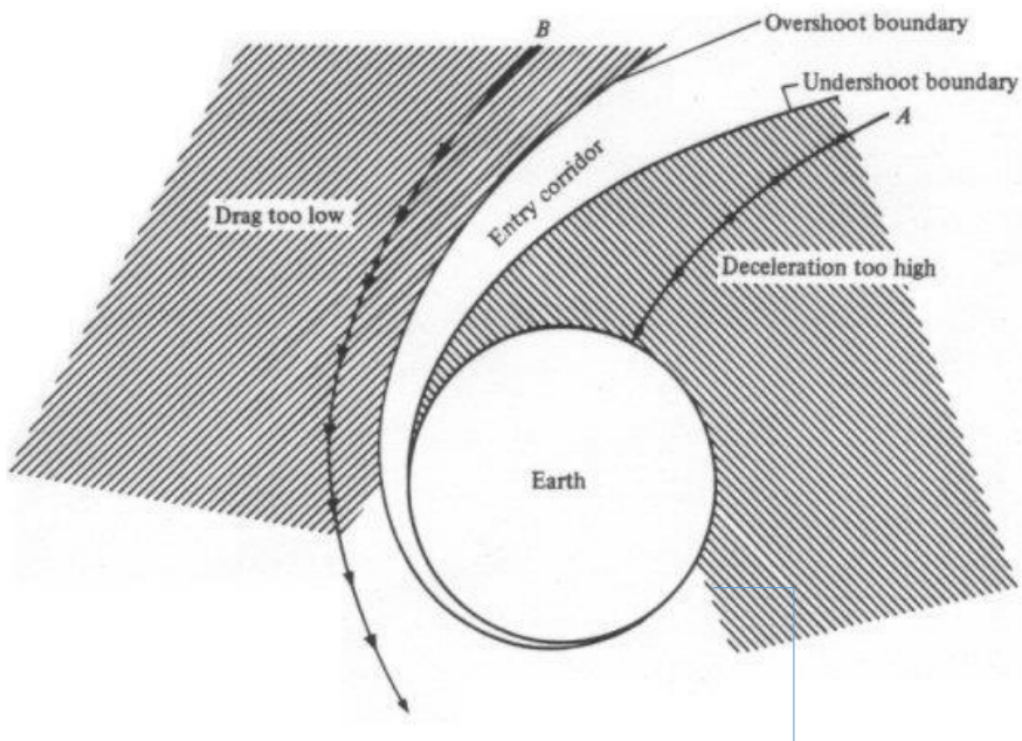


Figure 2.18: Re-entry path for Earth.

2.3.2 Blunt body entry vehicles

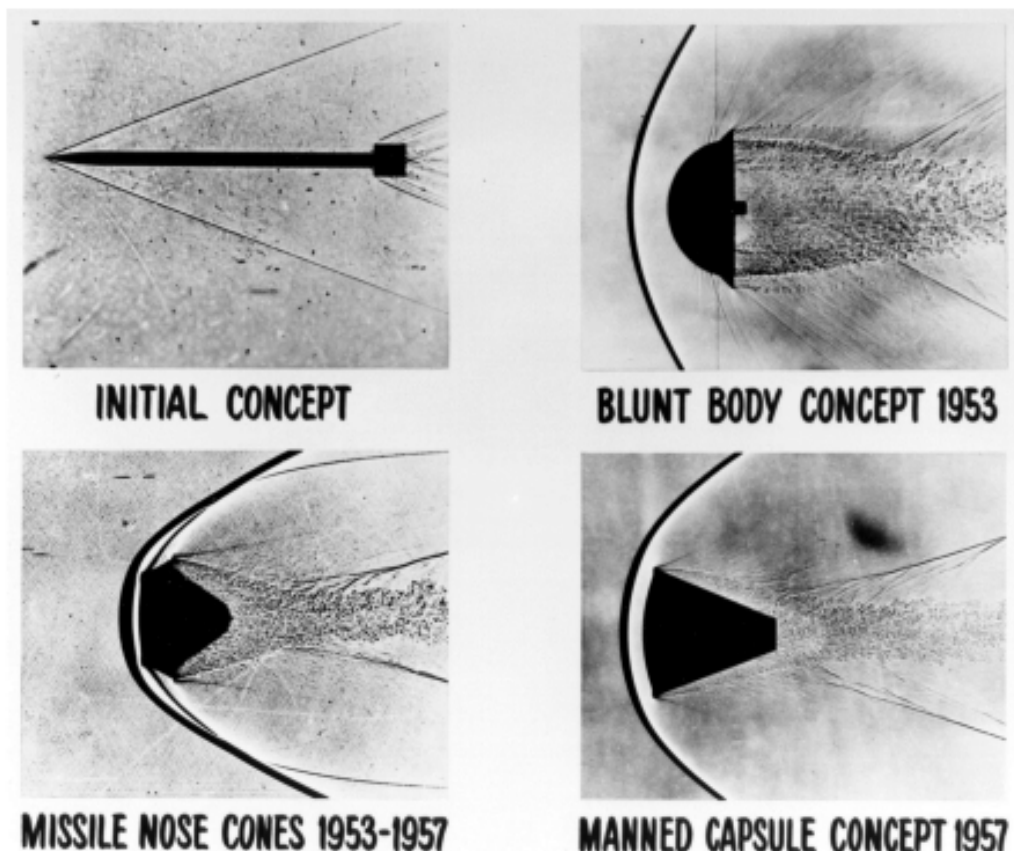


Figure 2.19: Re-entry path for Earth.

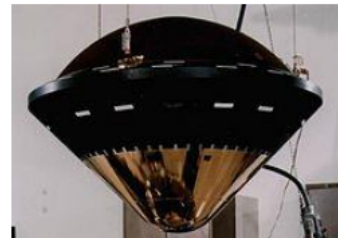
Allen & Eggers made the discovery that viscous heating decreases as the inverse square of the drag coefficient.

Shapes of entry types

- Cone



- Biconic



- Lower peak deceleration

Figure 2.20: Shapes of entry path.

2.3.3 Shock layer physics

Perfect gas model - breaks down at 500 K and not useable after 300 K (works okay for Titan because atmosphere is so dense and pressure high). Real gas model - requires table and inclusion of chemistry. Stagnation plane is about 0.14 times nose radius.

2.3.4 Different types of coatings

- SLA-561V stands for super light-weight ablator - used on all NASA mars missions, Starts to ablate at 100 W cm^{-2} but fails for heat fluxes greater than 300 W cm^{-2} . Peak value on Mars is 21 W cm^{-2}
- Phenolic impregnated carbon ablators - carbon fibre impregnated with phenolic resin. Low density with lowest conductivity. Worked well on Apollo mission capsules which entered at 12.4 km s^{-1} . Can withstand 1.2 kW cm^{-2}
- PICA-X - 10 times cheaper to manufacture than PICA
- SIRCA - silicon impregnated reusable ceramic ablators. Can be machined quite accurately.

Ablation layers

Thermal protection systems are used to protect spacecraft in space and during re-entry. Ablative heat shields displace shock and thermal boundary layer away from the wall. Two approaches:

1. Outer surface chars, melts and sublimes
2. Bulk of layer undergoes pyrolysis and expels product gases

The blowing is what displaces the boundary layers. (Note the similarity in last case with gas turbine engines). Pyrolysis can be measured in real time using thermogravimetric analysis, so that ablative performance can be evaluated. Ablation can also provide blockage against radiative heat flux by introduction carbon into the shock layer thus making it optically opaque. Radiative heat flux blockage was the primary thermal protection mechanism of the Galileo Probe TPS material (carbon phenolic). Carbon phenolic was originally developed as a rocket nozzle throat material.

2.3.5 Thermal soak

When pyrolysis does not occur, conductivity increases and heating occurs. All the TPS fail when the heating is reduced. Space Shuttle TPS tiles can withstand 1000 K one side and warm to the touch on the other side, but they are very brittle.

2.3.6 Cooling methods

- Passive - dump the heat shield at the last moment
- Actively cooling by radiating heat - e.g. hypersonic aircraft
- Feathered re-entry
- Inflatable heat shield

2.4 Conclusions

- Fascinating mixture of design and material selection
- Interesting overlap in the physics for both gas turbines and re-entry spacecraft